

Part 5

Synthetic Light Curves and Velocity Curves, Synthetic Spectra of Binary Stars and their Accretion Structures

Advances in Modeling Eclipsing Binary Stars in the Era of Large All-Sky Surveys with EBAI and PHOEBE

A. Prša¹, E. F. Guinan¹, E. J. Devlin¹, P. Degroote², S. Bloemen²
and G. Matijević³

¹Villanova University, Dept. of Astronomy & Astrophysics, 800 Lancaster Ave,
Villanova PA 19085, USA; email: aprsa@villanova.edu

²Instituut voor Sterrenkunde, K.U.Leuven, Celestijnenlaan 200D, B-3001 Leuven, Belgium

³University of Ljubljana, Dept. of Physics, Jadranska 19, SI-1000 Ljubljana

Abstract. With the launch of NASA's Kepler mission, stellar astrophysics in general, and the eclipsing binary star field in particular, has witnessed a surge in data quality, interpretation possibilities, and the ability to confront theoretical predictions with observations. The unprecedented data accuracy and an essentially uninterrupted observing mode of over 2000 eclipsing binaries is revolutionizing the field. Amidst all this excitement, we came to realize that our best models to describe the physical and geometric properties of binaries are not good enough. Systematic errors are evident in a large range of binary light curves, and the residuals are anything but Gaussian. This is crucial because it limits us in the precision of the attained parameters. Since eclipsing binary stars are prime targets for determining the fundamental properties of stars, including their ages and distances, the penalty for this loss of accuracy affects other areas of astrophysics as well. Here, we propose to substantially revamp our current models by applying the lessons learned while reducing, modeling, and analyzing Kepler data.

Keywords. methods: data analysis, methods: numerical, binaries: eclipsing, stars: fundamental parameters, stars: statistics

1. Introduction

A thorough understanding of the fundamental stellar parameters (masses, radii, luminosities, ages, chemical compositions and distances) and processes (energy transport mechanisms, nucleosynthesis, etc.) in stars across the Hertzsprung-Russell diagram is the core of stellar astrophysics. To rigorously study stars, we need to determine their properties as accurately as possible, using the minimum number of underlying assumptions. Eclipsing binary stars (hereafter EBs) are ideal astrophysical laboratories to achieve this goal: the favorable alignment of the line of sight with the orbital plane and the basic principles of classical dynamics that govern the motion of the components in a binary, reduce the determination of principal parameters to a simple geometric problem. This unique property, contrasted with other means of determining stellar radii that either apply to only a handful of objects (such as resolving the disk of a star) or are encumbered with a larger uncertainty (i.e. P - L - R relationships), promoted eclipsing binaries as key calibrators of stellar properties and distance gauges. Binarity allows us to determine the masses of individual components, and the alignment of a system's orbit with the line of sight and consequent eclipses allow us to determine their radii to better than a few percent (Andersen 1991). To perform such accurate modeling, both photometric and spectroscopic observations are required. An excellent overview of the state of the field is given by Torres, Andersen & Gimenez (2010).

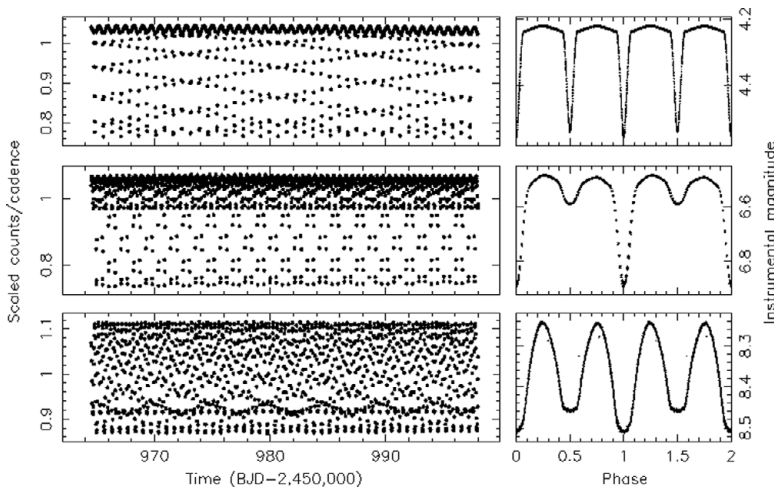


Figure 1. Kepler observations of a detached EB KIC 5513861 (top; $P=1.51012$ -d), a semi-detached EB KIC 8074045 (middle; $P=0.53638$ -d), and an overcontact EB KIC 3127873 (bottom; $P=0.67146$ -d).

NASA's Kepler mission (Borucki *et al.* 2010) revolutionized two crucial aspects of our ability for detailed EB modeling: the unprecedented photometric accuracy, and an essentially uninterrupted observing mode (cf. Fig. 1). Prša *et al.* (2011, paper I) and Slawson *et al.* (2011, paper II) cataloged 2165 EBs in the Kepler field found in the public Quarter 1 and 2 data, with periods ranging from an hour to several months. The EBs in the catalog are classified by morphology as overcontact, semi-detached, detached, and ellipsoidal. A preliminary analysis of these EBs was done by EBAI (Eclipsing Binaries via Artificial Intelligence; Prša *et al.* 2008), an approach based on back-propagating neural networks that yields principal parameters for all binaries. These estimates serve as a basis for detailed modeling.

Having superb quality data at hand has clear repercussions on our modeling capability. For the first time, we are observing astrophysical phenomena uninterruptedly, and to an amazing level of detail. State-of-the-art models such as the renowned Wilson-Devinney code (Wilson & Devinney 1971; Wilson 1979, 1993, 2007), ELC (Orosz & Hauschildt 2000), and PHOEBE (Prša *et al.* 2005) are showing systematics in a whole range of binary light curves. This is partly due to approximations embedded in these models, and partly due to missing and/or inadequate physics that has yet to be accounted for. Here, we identify the most striking deficiencies of our models that hinder the reliability and extensiveness of binary star solutions. Suitably rectified models allow us to determine fundamental stellar parameters to 1% or better. These are subsequently used to calibrate stars across the H-R diagram (Harmanec 1988), determine accurate distances (Guinan *et al.* 1998), and study a range of intrinsic phenomena such as pulsations, spots, accretion disks, etc. (Olah 2007).

2. Eclipsing Binaries via Artificial Intelligence (EBAI)

The EBAI project (Prša *et al.* 2008) employs backpropagating neural networks to rapidly estimate principal parameters from light curves. For many, Artificial Neural Networks (ANN) invoke a veil of suspicion, sometimes because they seem so intangible, at other times because they are a purely mathematical construct deprived of any physical

context. In reality, ANNs are very simple algorithms that hardly involve anything beyond summation and multiplication and are trained on a physical content.

In its basic form, an ANN is a system of three layers. Each layer consists of a given number of independent units. Each unit holds a single value. These values are propagated from each unit on the current layer to all units on the subsequent layer by weighted connections. Propagation is a simple linear combination $y_i = \sum_j w_{ij}x_j$, where x_j are the values on the current layer, w_{ij} are weighted connections, and y_i are the values that enter the subsequent layer. Before they are stored in their respective units, y_i are first passed through the activation function, A_f . This function, typically a sigmoid function $A_f(y_i) = 1/[1+\exp(-(y_i\mu)/\tau)]$, introduces non-linear mapping properties to the network. Coefficients μ and τ are selected so that $A_f(y_i)$ fall in the (1, 1) interval. This value is stored in the i -th unit on the subsequent layer. Layers in the three-layer network are usually denoted input, hidden, and output layer. In a nutshell, ANN is a non-linear mapping from the input layer to the output layer. In the domain of EBs, the ANN maps the input light curves to the output set of principal physical parameters. Training the network implies determining the weights, w_{ij} , on weighted connections. The back-propagation algorithm relies on a sample of LCs with known physical parameters; these are called exemplars. All LCs are propagated through the network and their outputs are compared to the known values. The weights are then modified so that the discrepancy between the two sets is minimized. This is an iterative process that needs to be done only once. After training, the network is ready to process any input LC extremely quickly. For example, solving 10,000 LCs on a single 2GHz processor takes around 5 seconds.

3. Physics Of Eclipsing BinariEs (PHOEBE)

Our current understanding of the properties and processes in binary stars shape our ability to model observed data. PHOEBE (Prša *et al.* 2005) is a physical model based on the Roche geometry; it includes more than 40 physical and geometric parameters that determine light and radial velocity (RV) curve properties. The most important effects implemented in the model are:

- an analytic description of binary star orbits, including apsidal motion;
- iterative solution of the Kepler problem that governs binary star dynamics;
- shape distortion due to eccentricity, tides and (asynchronous) rotation;
- radiative properties of binary star components, including gravity brightening, limb darkening and reflection effect;
- spots, circumbinary attenuation clouds, and third light.

Furthermore, PHOEBE provides minimization algorithms that fit the model curves to the data. This highly non-linear problem suffers from non-unique solutions: the *right* combination of the *wrong* parameters can fit the observed data very well. The algorithms currently in use, namely Differential Corrections (DC), Nelder & Mead (1965)'s Simplex method (NMS), Powell's direction set method, and genetic algorithms, have all met with success, but cannot be run robustly without experienced human intervention.

The level of detail in PHOEBE and its predecessor WD was sufficient for several decades, however this has been superseded by the Kepler mission. We are now seeing phenomena that have been theorized but never observed before, and we are seeing them systematically. The approach of modeling the EB baseline, while assuming that all neglected physical factors are buried deep in noise, is no longer applicable. The residuals are nowhere near Gaussian, and we cannot assume that these effects are only perturbations; rather, we need to account for their signatures in light and radial velocity curves rigorously.

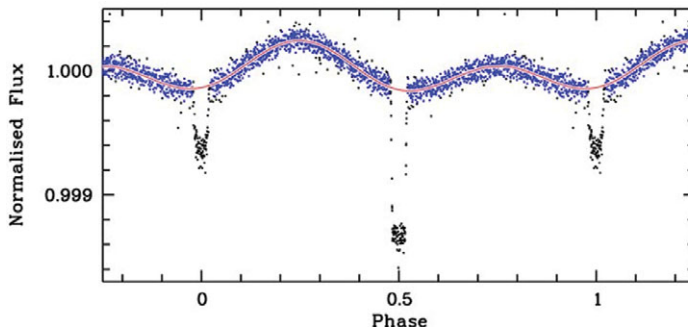


Figure 2. Kepler observations of KOI-74. The model fit consists of two sine waves, at the orbital and half-orbital period, corresponding to Doppler beaming and ellipsoidal variations, respectively. Adapted from Van Kerkwijk *et al.* (2010).

4. Challenges

In this section we present some of the challenges being addressed in the field of eclipsing binary stars.

4.1. Doppler Beaming

The required fidelity of models for EBs has been set historically by the photometric precision of ground-based observations, typically a few milli-mag per datapoint. MOST, CoRoT, and now Kepler, have attained a revolutionary photometric precision of several parts per million per datapoint. At this level, the photometric phenomenon of Doppler beaming was predicted to be observable (Loeb & Gaudi 2003). Doppler beaming (also boosting) refers to the shift in bolometric luminosity of a star accruing from its radial velocity. The resulting Doppler-shifted bolometric flux, F , is related to the stationary flux F_0 by $F = F_0(1 + 4v_r/c)$. At a given frequency ν , the observer sees $F_\nu = F_{\nu,0}(1 + (3 - \alpha)v_r/c)$, where α is a parameter that depends on the bandpass and the slope of the spectrum of the observed star. Essentially, beaming makes an object appear brighter on approach and fainter on recession, thus modulating the light curve of a binary system (cf. Fig. 2). Analogous to radial velocity information, disentangling orbital beaming in a light curve can yield the masses of the binary components.

Until recently, beaming was just a footnote for eclipsing binaries. However, the effect has now been detected for two Kepler binaries, KOI 74 and KOI 81, both likely white dwarfs (Van Kerkwijk *et al.* 2010), and for CoRoT-3, a massive planet/low-mass brown dwarf orbiting an F-star (Mazeh & Faigler 2010), as well as in a subdwarf B–white dwarf pair by Bloemen *et al.* (2010). Groot (2011) computed the observability of the rotational Doppler beaming effect for EBs, a photometric phenomenon directly analogous to the classical spectroscopic Rossiter-McLaughlin effect, which allows a photometric determination of the projected radial velocity of the eclipsed star as a function of phase. The effect is shown to be detectable for binaries ranging from double white dwarfs to massive O-stars, as well as for the WASP-33b-like transiting system, for which it could in principle reveal the host star’s rotational obliquity.

To date, most studies predicted and confirmed detections of Doppler beaming based on simplified, ad hoc theoretical estimates of the magnitude of the effect for binary stars (or star+planet). While this approach is adequate to confirm the expected physics, it clearly indicates the need to incorporate Doppler beaming, both orbital and rotational, into rigorous eclipsing binary models. Neglecting this effect would cause a substantial

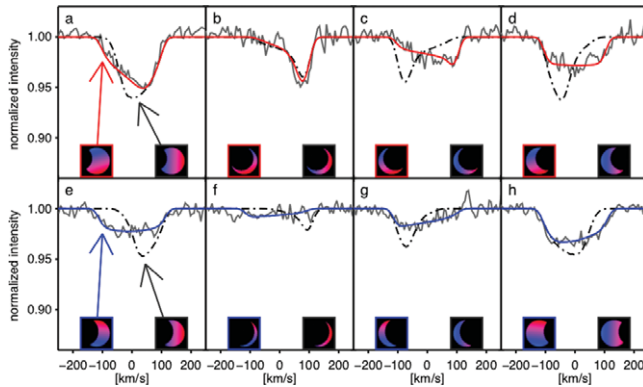


Figure 3. Comparison between observed spectra during the primary eclipse (top) and the secondary eclipse (bottom). Solid black lines are observations, the dash-dotted lines are the model fit of co-aligned stars, and the solid lines are model fits that allow for spin-orbit misalignment. Adapted from Albrecht *et al.* (2011). This is known as the Rossiter-McLaughlin effect, and has been observed in a number of stars and planets.

systematic discrepancy for objects of significantly different luminosities; for such objects, beaming provides constraints on RV semiamplitude without the need for spectroscopy.

4.2. Spin-Orbit Misalignment

Most current EB models are based on the Roche model, which assumes perfect alignment between the orbital and the rotational axes and handles each component's tidal distortion as due to the companion's point mass. However, careful ground-based studies have been able to discern that the components of close binaries in a number of systems show misaligned rotational and orbital axes (Albrecht *et al.* 2011). Observationally, this is most easily discerned via the Rossiter-McLaughlin effect, depicted in Fig. 3. The non-alignment of a host star spin-orbit has also been found for a number of hot Jupiters (Hebrard *et al.* 2008). Consequently, EBs and transiting exoplanets bring into question the initial conditions for the formation of both binaries and planetary systems.

The generalized Roche potential for binary systems, in which the stellar rotation is not aligned with the orbital revolution, is fundamentally different from the currently implemented co-aligned potential. Modifications to the potential have been derived by Limber (1963), Kruszewski *et al.* (1966), and Kopal (1978). The properties of the critical equipotential lobe and Lagrangian points for circular orbits have been studied in detail by Avni & Schiller (1982).

In binary star modeling, a Cartesian coordinate system is usually set at the center of the primary star, where x -axis points to the center of the secondary star, and z -axis points along the orbital revolution axis. Misalignment may be fully described by two angles: axial deflection from the z -axis (pitch), and rotation from the x -axis (yaw). The third angle (roll) may be dropped because of symmetry. A simple rotation of the coordinate system about the x -axis reduces this to a single-parametric problem, with a misalignment parameter θ' denoting the angle between the rotated z -axis and the spin axis, which due to the transformation now lies in the $x'z'$ plane. This one parameter determines the location and properties of the Lagrangian points, and hence the shapes of both components and instantaneous force fields acting on them (Avni & Schiller 1982).

A fully numerical search for equipotential surfaces in misaligned binaries needs to be implemented. These surfaces determine the shapes and radiative properties of components in binary stars. Since 3-D minimization is a computationally expensive task,

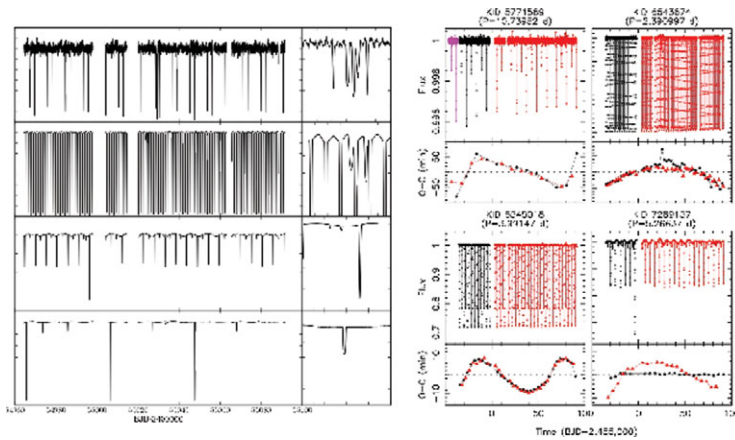


Figure 4. Left: 4 EB targets with tertiary events detected in the public Kepler data. These are indicative of tertiary components transiting the binary star. Right: eclipse timing variations for 4 interesting targets. Colors in the light curves denote data quarters (Q0: magenta, Q1: black, Q2: red), and primary and secondary eclipse timing variations (red and black, respectively).

the search will be initiated only when the misalignment parameter θ' changes its value. Equipotential surfaces will otherwise be stored for subsequent use.

4.3. Multiple Stellar Systems: Extranous Bodies in Binary Systems

In an EB, one would expect that primary eclipses and secondary eclipses are uniformly spaced in time. However, mass transfer from one star to the other, or rotation of the line of apsides (apsidal motion), or the presence of a third star in the system can give rise to changes in the orbital period, which in turn change the spacing in time between consecutive eclipse events. The eclipse times will no longer be described by a simple linear ephemeris, and the deviations from the linear ephemeris (usually shown in the O-C diagram) will contain important clues to the origin of the period change. Systematic measurements of the times of primary and secondary eclipses for the Kepler sample of EBs have been conducted (Orosz *et al.* 2011, Prša *et al.* 2012, in preparation). This is a tedious task, owing to a host of intrinsic variabilities and systematic problems. These include large spot modulations that may or may not be in phase with the eclipses, pulsations and/or noise in the out-of-eclipse regions, thermal events and cosmic ray hits that make the normalization of the light curves hard to automate, and eclipses falling partially or completely in data gaps. Fig. 4 presents some interesting cases of EBs with O-C variations evident in the public Kepler data.

The modeling codes can deal with the simplest case of apsidal motion, where the argument of periastron changes linearly in time ($d\omega/dt = \text{const.}$). We found, and successfully modeled, a number of EBs with strong apsidal motions, and the models successfully predicted the shapes of light curves without a substantial increase in systematics.

Our adopted model follows the basic concept laid out by Carter *et al.* (2011) that was applied to KOI-126, a hierarchical stellar triple system observed by Kepler. A hierarchical (or Jacobi) coordinate system is used when calculating the positions of the three bodies. In this system, r_1 is the position of star *A* relative to star *B* (the inner pair) and r_2 is the position of star *C* relative to the center of mass of (*A*, *B*). We may specify r_1 and r_2 in terms of osculating Keplerian orbital elements (period, eccentricity, argument of pericenter, inclination, longitude of the ascending node, and the mean anomaly). Newton's equations of motion, which depend on r_1 , r_2 , and the masses, may be specified for

the accelerations \ddot{r}_1 and \ddot{r}_2 (Soderhjelm 1984; Mardling & Lin 2002). An additional term may be added to the acceleration of r_1 due to the post-Newtonian potential of the inner binary (Soffel 1989). Further perturbing accelerations may be added to the acceleration of r_1 corresponding to the non-dissipative equilibrium tidal potential between stars A and B and the potential associated with the rotationally-induced oblate distortion of stars A and B (Soderhjelm 1984). In this approximation, the axial spins of stars A and B follow the evolving orbit, staying normal to the orbit and spinning at a rate synchronous with the orbit. Both the accelerations due to tides and rotations depend on r_1 , the masses, and the radii of both components. The acceleration due to rotation also depends on the angular axial spin rate of both stars A and B . The spin rates and apsidal constants are assumed to be the same for both stars. This system provides a coupled system of differential equations that are solved using the Bulirsch-Stoer algorithm. The positions of the three objects are then projected to the barycentric plane, which is necessary to account for the finite speed of light and predict eclipse timing variations. Carter *et al.*'s method assumes spherical stars, whereas our implementation will feature tidally deformed stars whose shapes will be derived from the generalized Roche formalism presented in the previous section.

4.4. Markov Chain Monte Carlo heuristics and Bayesian Error Estimates

Perhaps one of the worst plagues of EB modeling is the inherent non-linearity of the parameter space and thus a high degree of solution degeneracy. Coupled with that is a classical approach to data fitting by least squares and estimating errors from the covariance matrix. This has two important and dire consequences. First, essentially any minimizer used is bound to get stuck in local minima. Ways around this have been proposed, most notably by heuristic Monte Carlo scanning and parameter perturbations (Prša *et al.* 2005; Prša & Zwitter 2007), or by utilizing global search algorithms such as the Metropolis-Hastings simulated annealing, which, however, dramatically increases computing time. Second, chi-square fitting is done on a data curve level rather than on the parameter level. Any deviation between the model and the data will penalize all parameters marked for adjustment. To see why this is problematic, consider adjusting the semi-major axis or the mass ratio of a well detached binary. There is absolutely no information contained in a light curve on either of the two parameters; all information lies in radial velocity curves. Hence, if a simultaneous LC+RV least squares fit is employed, the minimizer will fit the correct RV signature for the two parameters, but it will essentially fit numerical noise in the EB light curve. The number of data points in a light curve is typically an order of magnitude larger (several orders in case of Kepler), so the determination of these two parameters will be heavily weighted towards light curves where there is little to no oversight when determining their values.

Markov Chain Monte Carlo (MCMC) proves to be a powerful tool for Bayesian inference because it provides more statistical information and makes better use of data than chi-square fitting. The goal is to determine what configurations of physical and geometric parameters are consistent with given light and radial velocity observations. For each parameter, we provide an initial estimate – a prior – that does not need to be close. After running a given set of chains, MCMC returns a posterior distribution for each parameter: a histogram of attained values that determines the most likely value as well as the uncertainty in the statistical sense. Thus, MCMC provides a best-fit solution and the corresponding error estimates by assessing them on a parametric level rather than on a data-set level. The latter is exactly the culprit that we would like to eliminate, and MCMC is a clear path to doing so. The approach has been implemented and used successfully in BLENDER (Torres *et al.* 2011), a tool devised to discriminate between

bona fide extra-solar planets and background EBs in the Kepler data-set. Other examples of a successful MCMC application include (Bloemen *et al.* 2010) for Doppler beaming, and Hou *et al.* (2011) for fitting radial velocities of stars that host extra-solar planets.

5. Conclusion

Ultra-high precision space missions MOST, CoRoT, and Kepler revolutionized observations, and our tools need to keep up with them. The two striking issues are: (1) the amount of data acquired and in need of automated processing, and (2) the inadequacies of our models that cause systematics in the solutions. Both need to be addressed immediately, otherwise our analysis capabilities will be inferior to the data. To address the first issue, we propose to use the artificial intelligence based engine EBAl; for the second issue, significant effort in restating the physics and geometry of the model is underway.

References

- Albrecht, S., *et al.*, 2011, *ApJ*, 726, 68
 Andersen, J. 1991, *A&ARv*, 3, 91
 Avni, Y. & Schiller, N. 1982, *ApJ*, 257, 703
 Bloemen, S., *et al.*, 2010, *MNRAS*, 407, 507
 Borucki, W. J., *et al.*, 2010, *Science*, 327, 977
 Carter, J., *et al.*, 2011, *Science*, 331, 562
 Groot, P. J. 2011, *arXiv*, 1104:3428v3
 Guinan, E. F., Fitzpatrick, E. L., & Dewarf, L. E., *et al.*, 1998, *ApJ*, 509, L21
 Harmanec, P. 1988, *Bulletin of the Astronomical Institutes of Czechoslovakia*, 39, 329
 Hebrard, G., *et al.*, 2008, *A&A*, 488, 783
 Hou, F., *et al.*, 2011, *arXiv* 1104:2612
 Kopal, Z. 1978, *Dynamics of Close Binary Systems*, ISBN 9-789-02770-820-5
 Kruszewski, A. 1966, *Adv. Astr. ap.*, 4, 233
 Limber, D. N. 1963, *ApJ* 138, 1112
 Loeb, A. & Gaudi, S. B. 2003, *ApJ*, 588, 117
 Mardling, R. A. & Lin, D. N. C.. 2002, *ApJ*, 573, 829
 Mazeh, T. & Faigler, S. 2010, *A&A*, 521, L59
 Nelder, J. A. & Mead, R. 1965, *Computer Journal*, 7, 308
 Olah, K., *IAUS*, 240, 442
 Orosz, J. A. & Hauschildt, P. H. 2000, *A&A*, 364, 265
 Prša, A. & Zwitter, T. 2005, *ApJ*, 628, 426
 Prša, A. & Zwitter, T. 2005, *ASPC*, 370, 175P
 Prša, A., *et al.*, 2008, *ApJ*, 687, 542
 Prša, A., *et al.*, 2011, *AJ*, 141, 83
 Slawson, R. W., *et al.*, 2011, *AJ*, 142, 160
 Soderhjelm, S. 1984, *A&A*, 141, 232
 Soffel, M. H. 1989, *Relativity in Astrometry, Celestial Mechanics and Geodesy*, ISBN 3-540-18906-8
 Torres, G., Andersen, J., & Gimenez, A. 2010, *A&ARv*, 18, 67
 Torres, G., *et al.*, 2011, *ApJ*, 727, 24T
 Van Kerkwijk, M. H., *et al.*, 2010, *ApJ*, 715, 51
 Wilson, R. E. & Devinney, E. J. 1971, *ApJ*, 166, 605
 Wilson, R. E. 1979, *ApJ*, 234, 1054
 Wilson, R. E. 1993, *New Frontiers in Binary Star Research*, 38, 91
 Wilson, R. E. 2007, *IAUS*, 240, 188